PÁZMÁNY
Pázmány Péter Catholic University
Faculty of Information Technology and Bionics

Tutored Research Project I.

Artificial intelligence-based sensor system for water rescue and disaster management

Csatári, Dominik
Computer Science Engineering MSc

Supervisor: Dr. Cserey, György Gábor

2023

Declaration of Authenticity

I, the undersigned Dominik Csatári, student of the Faculty of Information Technology and Bionics at the Pázmány Péter Catholic University, hereby declare that I have prepared the present Tutored Research Project myself without any unauthorized help, and that I have only used the sources specified in the Tutored Research Project. I have clearly marked all parts that I have literally taken from other sources or have rewritten or translated while keeping the meaning of the original text, also indicating the source thereof. I have not submitted this Tutored Research Project to any other study programs.

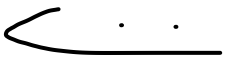

Dominik Csatári

Abstract

In this Tutored Research Project the aim was to create well-founded background for future development of an artificial intelligence-based sensor system. This included a research in similar literature. To tackle the issues highlighted in these papers, I have created several experiments aimed at a methodical comparison of my findings with theirs. The project's central challenge involves estimating the Echo Excess value (from the sonar equation) in ultrasound imaging systems, particularly considering complications arising from transmission losses in challenging conditions like high turbidity and increased flow rates. The experiments successfully demonstrated the system's functionality, confirming the effectiveness of tested scripts and equations. Measurements in turbid water conditions revealed consistent results, addressing concerns raised in scientific literature.

Contents

Chapter 1

Introduction

1.1. Background

This Tutored Research Project is motivated by the sinking of the cruise ship Hableány in the Danube, and aims to implement a system that will make it much easier to locate and rescue victims in a disaster, even in difficult circumstances. The whole of this project, is to create such a system. The whole project consists of more phases. The scope of this semester was to provide a solid background of the statements we make based on scientific literature.

In the field of waterborne disaster management, sonars (sounding devices), currently used on submarines or as a stand-alone device, are used to map the topography of lakes, rivers and seas, but are also used to locate static or moving objects at sea [1]. At greater distances (depths) and pollution, even extremely high illumination does not make the environment suitable for observation with a conventional camera. With current methods (sonar), a depth/relief image of the current state of the bottom or seabed can be taken, shown to the diver, who then has to navigate in the water from memory, essentially without orientation information. In strong currents, objects with dangerous and essentially unknown geometry are approached blindly by groping, relying only on memory for information from the previously recorded image. This makes rescue dangerous, slow and difficult. It would be necessary for the diver to have continuous and up-to-date visual information about the area or object concerned, according to his current orientation, even during the rescue.

Moving forward, we can use the gathered knowledge, to create an artificial intelligence sensor system, providing an augmented reality based 3D map, for a diver to see the

surrounding environment even when no light source is available. As our sensor system is sonar based, our measurements will be mostly ultrasonic signals. One of my first task was to specify in which cases can our model work. To be more specific, in this semester my goal was to:

1. Collect relevant literature to enhance understanding and establish a solid foundation for the project.
2. Elaborate on the physical specifications of such a model and define their boundaries.
3. Develop laboratory experiments tailored to specific specifications if required.
4. Sum up the experiment results and explain how they affect the project.

1.2. Outline

The summary of the chapters of my Tutored Research Project:

Chapter 2 This chapter summarizes the existing research and necessary background information to grasp the problem we're addressing.

Chapter 3 In this chapter, I document the methods employed and provide an overview of how they generally function.

Chapter 4 In this chapter, I present the results obtained from the experiments conducted using the designed experimental setup, supported by relevant figures.

Chapter 5 In this chapter, I provide a summary of the results obtained and discuss future plans.

Chapter 2

Related Works

2.1. Sonars

2.1.1 Introduction of echo sounders

Sonar is commonly used as an echo sounder which in general terms means a device, which is able to track or map the bedding with ultrasonic waves under a body of water. In this general setting, these kind of echo sounders had been in use for more than half a century now [1]. For deciding upon the depth or the distance we need to travel till the bedding, a so called Single Beam Echo Sounder is useful. As the name suggests it is such a hydrographic surveying device, which uses only a single, acoustic beam. These kind of echo sounder's structure might be built with the following components:

- **Transducer:** These devices have a piezoelectric transmitter which generates mechanical energy (ultrasound) from an electrical signal. They also have a receiver part, which is able to convert ultrasounds into an electrical signal which can be later processed. Usually the same piezoelectric element processes the signals both way.

- **Pulse Transmission:** The generated pulse is sent out and after that, the device waits for the return of an ultrasound from the bedding or elsewhere. This is usually compared to a conversation structure's having a "speaking" and "listening" part.

- **Reflection:** when the ultrasound wave hits the bedding a part of the energy is absorbed, part of it is scattered and part of it is reflected back, which can be

detected with the transducer. It has a lower amplitude, regarding the sent out signal. This returned signal is called an echo.

If we measure the time from transmitting an acoustic beam and receiving one with an amplitude above a given threshold, we are able to calculate the time of flight of the original ultrasound wave. With this we can calculate the distance with the following formula. [2.1] The speed of sound in water is calculated as 1500 $\frac{m}{s}$ [2].

$$\text{Depth} = \frac{\text{Speed of Sound} \cdot \text{Time of Flight}}{2} \tag{2.1}$$

2.1.2 Frequency

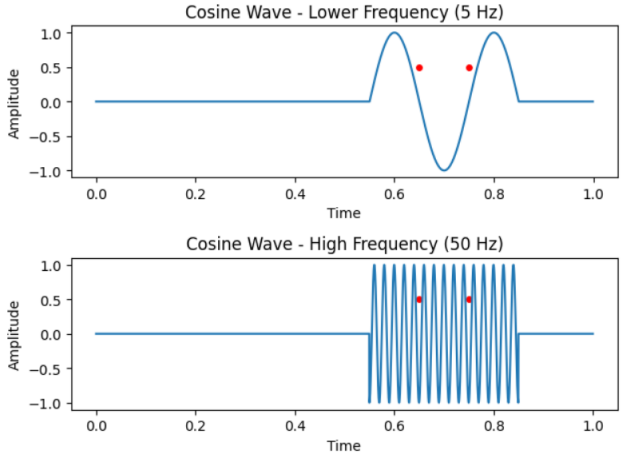

Figure 2.1: Two cosine waves showing 1-1 wave packets. The top, having a frequency of 5Hz and below it one with 50Hz. A red dots are added on both function at the same positions.

In ultrasonic devices, the number of emitted waves over a time period is quantified with the measure of frequencies. These devices are mostly used in a range from 20kHz up to several MHz even GHz in some applications. As for visualisation I have created a figure which shows how one wave can detect two different points in the same troughs not having any crest separating them.[2.1] This is the case for wave having a smaller frequency. That is why wavelengths can be associated with the resolution of a imaging process. Longer wavelengths (lower frequencies) produce poorer resolutions. In Figure 2.1 the wave in the upper plot cannot distinguish between the two red scatterers, while the response of the lower wave would produce two separable reflection peaks. However, high frequency waves scatter more, meaning that higher ratio of its energy gets absorbed, limiting the

range they can insonate. This exchange between parameters can be understood more easily, telling different kind of resolutions apart.

Resolutions

As ultrasonic devices can be utilized for different types of tasks, it is important to generally define the area you decide to use it in. You can emphasize different needs, for example range resolution. By this term we generally mean the capability of telling two detection points apart which are close to each other. If these targets are in the same beam line, range resolution is formulated by the following equation [3][4].

$$\text{Range Resolution [m]} = \frac{\text{Speed of Sound [m/s]} \cdot \text{Pulse Length [s]}}{2} \tag{2.2}$$

Usually the transmitted ultrasound (because of its finite length) does not consist of a single frequency. It can be better described by a range of frequencies, the bandwidth. This results in an ambiguous pulse length, which is more detectable at higher frequencies. We can derive a connection between the frequency span of the signal (called bandwidth) and the range resolution from the [2.2] equation knowing, that

$$\text{Pulse Length (Range)} = \frac{1}{\text{Bandwidth}}. \tag{2.3}$$

Therefore, if we lower the Pulse Length, we would get a better resolution, but also this comes with the cost of having a wider bandwidth, limiting the precision of the measurement [4].

Also, if we are using a multibeam sonar system, we might consider to account for having a great angular range resolution as well. In general, if the target is further away, it is harder to receive accurate information about its position. As the width of the beam is inversely related to the frequency, we can state that a narrower beam would result in a better angular resolution. Diving deeper, we can see that this resolution has a more complex relationship with the setup of our device, namely the beamforming part. Beamforming is the process of optimizing and focusing our ultrasonic energy to a given range. In this process we develop a main lobe, where the concentrated energy is. Note, that every array system has side lobes, it is the matter of optimizing the arrangements [1][2][5].

2.1.3 Array-based Sonar Mapping Systems

As mentioned in section 2.1.2, there are array-based mapping systems, providing greater opportunities for mapping purposes. We can distinguish two major types. Sidescan sonars

and Multibeam Echo Sounders, MBES for short. Both techniques have a wide range of usage, as both of them promise a great resolution, having enough transducer elements. As for mapping the bedding, MBES provides a less rigid configuration, meaning the way the beamforming is chosen can be dependent by the current environment, giving us an adaptive parameter to work with. Considering our implementation, MBES technique seems more viable [1].

2.2. Environment Considerations

Knowing how your sonar performs can mostly be determined in practice. However, there are some well-founded connections and mathematical formulas that can provide an estimation on the penetration and propagation capabilities of the device.

2.2.1 Sonar Equation

All sonar's have a level of capability of detecting targets. This form of general performance can be expressed with the sonar equation [1][4].

$$\mathrm{EE} = \mathrm{SL} - 2\mathrm{TL} - (\mathrm{NL} - \mathrm{DI}) + \mathrm{BS} - \mathrm{DT} \tag{2.4}$$

Where **SL** = source level, **TL** = transmission loss, **NL** = noise level, **DI** = directivity index, **BS** = bottom backscattering strength and **DT** = detection threshold. **EE** stand for Echo Excess which is the measure of echo detection.

Most of these factors can be countered in a well design setup, or be realised adaptively. For example **BS** can change depending on the surface it backscatters from. However, the **TL** value is highly correlated with the environment's factors, such as temperature, salinity, pressure and density. As these factors are mostly deterministic (only small changes are likely), it would be preferable to know beforehand their effect on our Echo Excess [4].

2.2.2 Temperature

In a more general setting we can raise the question, how does temperature affects the speed of sound? If it is severe, we would account these effects with some parameter optimization. As shown in several papers the accountability of these changes are quantifiable, meaning it is simple to adjust our settings, our model for seasonal changes in the water temperature [6][7]. Note, that this statement is true for smaller body of water (river, lake,

or some small area of the sea), as in the ocean with larger water columns the behaviour of temperature becomes more complex [4].

2.2.3 Salinity

Salinity is the measure for dissolved salts and minerals in the water. Although it is an important variable to keep in mind it is an easily accountable measure in case of our study. Other studies have shown that the effect of salinity has the least significant impact on the speed of sound [7].

2.2.4 Turbidity

Turbidity of the water can be described as the measure of its relative clarity. It resembles an optical characteristic; however, it also serves as a measure of suspended particles in the medium. Turbidity is measured in in NTUs, which means "Nephelometric Turbidity unit". The higher this measure the less clear the water is. In general we know, that tap water is less than 5 NTU, ideally below 1, while milk is around 4000, having minimal transparency.Since the conditions in rivers and lakes are not ideal, we need to find out if ultrasonic devices can be used in water with high turbidity [7].

In a study [7], there were three cases of turbidity effect studies, differing on their depth and turbidity level, in a range of 94.5 cm to 128 cm and a concentration from 39 to 525 NTU. Also for some cases the flow of the water was considered, as it might have a substantial impact on the measures. In this study they found that still turbidity has little to no effect on measuring the bedding in neither of the cases. However, when we try to measure the distance from the bed in this turbid water with the water flowing, we see errors occurring. The errors get worse when increasing the flow of the water. with the Velocity of the water changing from $4\frac{cm}{s}$ to $9\frac{cm}{s}$, The Relative Depth Error increases from 4% to almost 8%, independent by the given NTU measures. Note, that in the study at higher velocity the results seem to have smaller error. That is only because of the sonar device's tolerance, it is not able to locate the bed at this point. So, when the turbidity measurements are above a certain threshold, the NTU level does not matter much; the error is mainly caused by how the water flow distributes it.

Chapter 3

Methods

After reviewing scientific papers in Section 2 to identify potentially questionable or crucial findings, I have selected specific tasks for experimentation in a well-designed laboratory setup. The aim is to generate our own results, allowing for comparisons with findings in other papers. The main tasks were to build a model where with a transducer we can measure the distance from the transducer to the bottom, and process the reflected signal. After this, we have created several setups including tests for turbidity and water flow.

3.1. Signal Processing

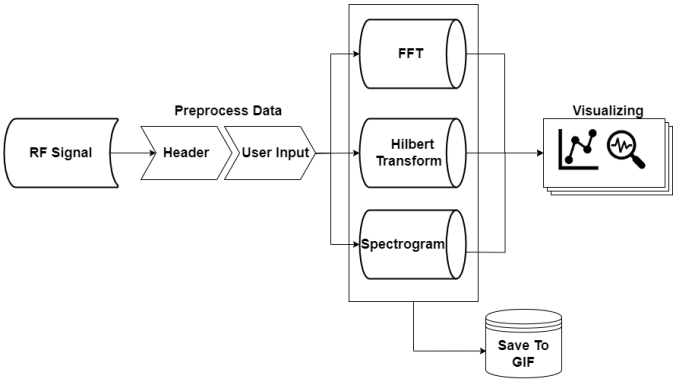

Figure 3.1: Flowchart of the Python script for processing transducers signal

The signal we detect with a transducer is a raw radiofrequency (RF) signal, showing different strength and intensities on the y-axis, and having the Time domain in its x-axis. As an active transducer process has a transmitting and receiving phase, we are only interested in signals happening after a well-defined time period, as at the start of the RF signal it is usual to have false amplitudes due to the switching between phases.

In addition, it is needed to transform the signal from time domain to frequency domain, as many of the information can only be read from those. Gathering these needs, I have designed a simple script for visualising and processing incoming signals.[3.1]

3.1.1 Data Preprocessing

Upon receiving data from the transducer, the necessary steps involve transforming it into a coherent format for effective utilization in signal processing. During a measurement, we first transmit an ultrasonic wave, than we save out a received signal digitized at a given sampling rate, till the end of the measurement. The system can save transmit-receive datalines at 1 s intervals. One line of measurement data would have the following specifications.[3.1][3.2]

$$\text{Sampling Time [s]} = \frac{1}{\text{Sampling Frequency [Hz]}}. \tag{3.1}$$

$$\text{Receiving Period [s]} = \text{Buffer Size} \cdot \text{Sampling Time [s]}. \tag{3.2}$$

This gives, that in a 1 second period we save out a single receiving period, from $PulseRepetitionFrequency = \frac{1}{ReceivingPeriod}$ many created. Additionally, we are able to calculate the distance from the transducer to the bottom and the Time of Flight with the equation 2.1 and 3.1, having that we can detect peaks in our signal.

In the saved .csv data, the table features a header as its first row, with values indicated by bold text corresponding to the following sequence: **USUT - TX channel number - Buffer Size - RX channel number - Sampling Frequency - Values Bit Number (8 or 12)**. After this, every row is one received signal line, with values in 8 or 12 bits. Given that the typical buffer size falls within the range of 8000 to 32000 and the sampling frequency can vary from 1.25MHz to 160MHz, it's conceivable to have thousands of measurements within a second. The values in the script are rescaled from their original range between 0 and 1 for better understanding. Through user input, we can specify a value for post-delay, allowing for adjustments to the original measurements that may have a cutoff at the beginning of the signal [8].

3.1.2 Hilbert Transform

As mentioned in Section 3.1.1, we need a method for finding peaks in our signal, so we can detect targets. The target in our case is the bedding. The received RF signal at

a reflection point reflects the whole transmitted wave package with around 10 periods of a sine wave. For an efficient peak detection first the envelope of the signal should be extracted. For this we can use the Hilbert transform, where the magnitude of the analytical signal gives an envelope. For this implementation, I have used a scipy libary [9] with the function *scipy.signal.hilbert(x)*, where 'x' is the signal data.

3.1.3 FFT

The Fast Fourier Transform (FFT) algorithm allows us to compute the discrete Fourier transform, transforming an original RF Signal from the time domain to the frequency domain. This numerical conversion provides insight into the predominant frequencies present in our signal. In Python, the numpy library facilitates this process [10]. Utilizing the function *np.fft.fft(a)*, where 'a' represents the amplitudes of the RF signal. It is important to note that the result is complex. When plotting the results with corresponding frequencies, it is necessary to depict the absolute value of the transformed data.

3.1.4 Spectrogram

Concerning the signals, our objective is to demonstrate that at specific timestamps where we observed amplitudes, the content of the measurement corresponds to the transducer's frequency. For this I have used a transformation of the signal with the help of spectrograms, as they visualize the frequency content across different time intervals. For this, I have used scipy libary with the function *scipy.signal.spectrogram(x,fs,window)*, where 'x' is the time series of measurement values, '*fs*' is the sampling frequency, and *window*, set to a Gaussian Window [11]. With this window we can look at the FFT results at sized intervals, leaving us with smoother visualization.

3.2. Laboratory Experiment Design

In these measurements, our goal is to conduct our own experiments, enabling us to compare our results with those discussed in Chapter 2. For this I have designed the following:

1. Demonstrating the workflow, showcasing the application of the described equations, the script, and adherence to the transducer's specifications.
2. Measurements in turbid water.
3. Measurements in turbid and flowing water.

3.2.1 Demonstrating the workflow

For demonstrating the workflow, we have designed a setup, where we have used a transducer, with a stand attached to it, on which we could precisely set the distance. After setting the distance, we started the measurement, than we gradually increased the distance, while saving out received signals accordingly as described in 3.1.1. With the help of the script and the equations described in Section 3.1.1 and in Chapter 2, we would be able to compare our results to the actual distances. Furthermore, on the spectrogram we have created, we aim to identify the transducer's frequency, providing evidence for our approach. In future this could also provide a mean to accurately measure the flow rate utilizing the Doppler effect [12].

For a transducer, we have used two different devices. First a 4MHz single-element transducer produced by MediCad, connected with a Ultrasonic Pulser/Receiver and Analog to Digital Converter, named EUT3160(T) [8]. The setup of the measurement was configured in the software, EUT3160 provided. The second transducer, Sonostar L6C was a wireless linear 10MHz, 192-element array, with the available WirelessUSG software.

3.2.2 Measurements in turbid water

For the turbidity test, we have used talcum powder, as suspending particles for decreasing the water's transparency, increasing its absorption rate. We have worked above a limit where the water was not transparent anymore. Quantitatively it meant, we had worked above the NTU level, according to the paper [7] mentioned in Chapter 2. With this prepared, I have repeated the same process as before (in Section 3.1.1).

3.2.3 Measurements in turbid and flowing water conditions

In this part of the experiment, I needed to create turbulent and directed flows in the water. For this, I have created the setup shown in Figure 3.2. For the measurement I have used a water pump, capable of generating 2000 $\frac{l}{h}$ water circulation. Following this, by using food coloring, I could detect turbulent flows, enabling me to adjust my setup accordingly. In this configuration the transducer was set still, so any further changes in the distance estimation would be written as an error. The target **3)** on Figure 3.2 has a ball like structure. This was necessary as the single-element transducer is highly angle-sensitive, detecting beams only on a perfectly perpendicular path. The sphere-like object reflects the beam in many directions, including the perpendicular one. Angle θ, marked **8)** in Figure 3.2, should not equal 90°, as the wireless ultrasound **4)** calculates

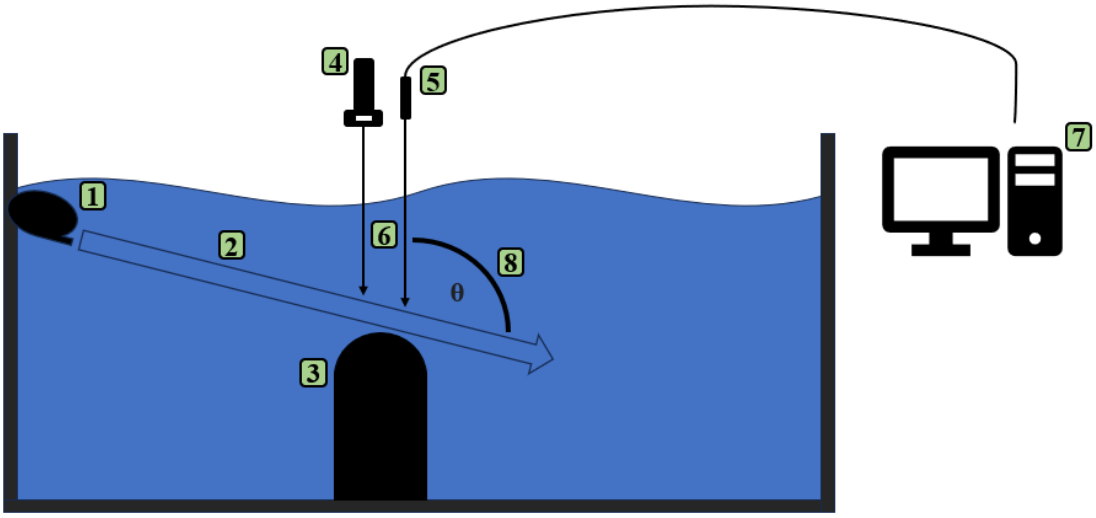

Figure 3.2: Shematic figure of the measurement's setup, where **1)** is the water pump, **2)** is the directed flow, **3)** is the target, **4)** is the wireless ultrasound Sonostar L6C, **5)** is the transducer, **6)** is the direction of the measurement, **7)** represents the software, **8)** is the angle between **2)** and **6)**.

Doppler frequencies which is indeterminant at that angle according to the equation 3.3.

$$\mathrm{V} = \frac{\mathrm{C(Fs - Ft)}}{\mathrm{2Ft(cos}\theta\mathrm{)}}. \tag{3.3}$$

Where V is the calculated velocity, C is the speed of sound, *(Fs-Ft)* is the Doppler shift, Ft is the transducer's frequency and θ is the Doppler angle. Furthermore, the wireless ultrasound, will also give us a feedback whether there was a Doppler shift, due to the flow of turbid water or not.

Chapter 4

Results

In this chapter, I am going to share the results that had been measured in experiments that were designed accordingly to Chapter 3.

4.1. Demonstrating the workflow

The first experiment was done in a small container made of acrylic glass, having a size of 5 cm × 5 cm × 8 cm with its height being 8 cm (not filled with water to the brim). I have worked with the following parameters, using the single-element transducer:

- **Transducer's frequency:** 4MHz
- **Sampling Frequency:** 160MHz
- **Time Period:** 40s
- **Buffer Size:** 10000
- **Value's Bit Size:** 12
- **Post Delay:** 0

In the script I have saved out the first received signal and the last, which was the 40th row. Then, I have transformed both with Hilbert Transform, generating high magnitudes so received signals are easily distinguishable. This process is shown on Figure 4.1. Note, that the x-axis is already modified with the equation 2.1, so the distance is the actual distance of the the transducer and the bottom of the glass. On the *first transformed signal* the first peak is at **29.74 mm** and the second at **32.34 mm** which corresponds to the thickness of the glass bottom. These distances are kept in case of the *last transformed signal* as well. Peaks in this signal are at **41.99 mm** and at **44.6 mm**. The distance of

the first peaks between the corresponding signals is 41.99 mm − 29.74 mm = **12.25 mm**. These distances support the measurements we have measured with rulers. Also, the spectrogram of the signal, as seen in Figure 4.2, indicates a higher value at 4MHz, supporting our initial statement.

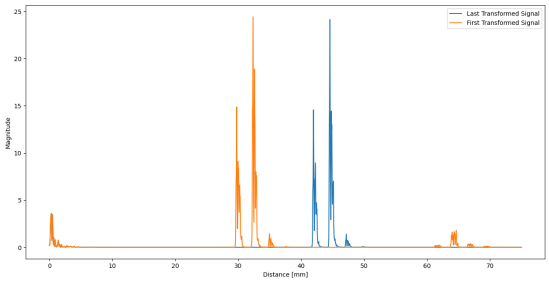

Figure 4.1: Hilbert Transform of Signal measured in 4.1 measurement. Orange is the first Transformed Signal, Blue is the last.

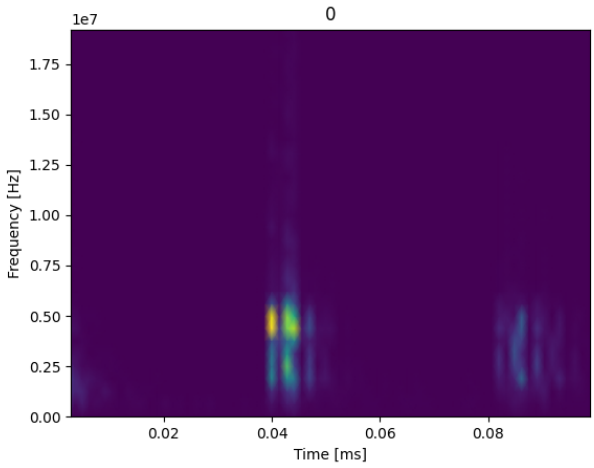

Figure 4.2: Spectrogram of the first measurement measured in measured in 4.1. The '0' on top of the figure indicates, it is the first received signal.

4.2. Measurements in turbid water

For the second measurement I have used talcum powder to decrease the transparency of the water. For this I have created a similar setup, with only some parameters differing:

- **Transducer's frequency:** 4MHz
- **Sampling Frequency:** 160MHz

- **Time Period:** 44s
- **Buffer Size:** 16384
- **Value's Bit Size:** 12
- **Post Delay:** 0

The buffer size was saved with 30000 samples in one received signal, however conversion of the *.csv* file cut off the columns at the end of it. This has no impact on the measurement, as neither of those numbers contained valuable information (having no received signals). The process went similarly, and the pulses were recognizable at the given distances. However the results and the signal in itself was noisier, as shown on the figure 4.3 and 4.4. Note, that they are compared regarding their noise level. Their distance from the transducer is not a relevant information in this case, as these figures represent different timestamps. About the frequencies, the spectrogram of this measurement still indicates the original 4 MHz signal. I have attached a figure regarding the spectrogram in the Appendix at B.1.

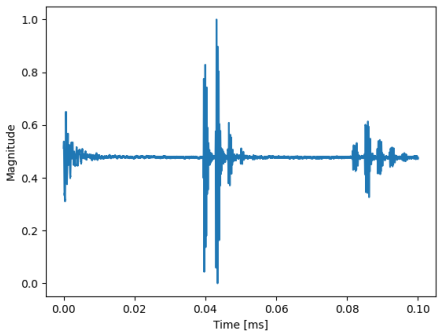

Figure 4.3: RF Signal of the measurement in Section 4.1.

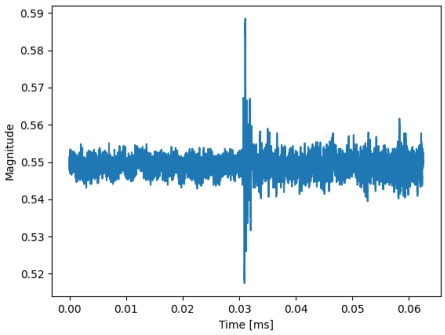

Figure 4.4: RF Signal of the second, noisy measurement in Section 4.2.

4.3. Measurements in turbid and flowing water conditions

In this third experiment, we have arranged the the setup according to the Figure 3.2. I have used the following parameters:

- **Transducer's frequency:** 4MHz
- **Sampling Frequency:** 40MHz
- **Time Period:** 448s and 76s

- **Buffer Size:** 10000
- **Value's Bit Size:** 12
- **Post Delay:** 0

For the first part we measured the initial distance shown by the RF signal plotted with distance in mm on the x-axis. Than, we turned on the water pump at the angle. This is the 448 s interval of this section. I plotted the measured and calculated Hilbert transform of the first and last received signals to check for any visible errors caused by the directed flow of the medium. The results are shown on Figure 4.5. There is no visible changes between the first and last received signal, meaning there is no error caused by the flow itself. Only small changes are shown on the amplitudes, but when no wave packet was detected neither signal made any errors.

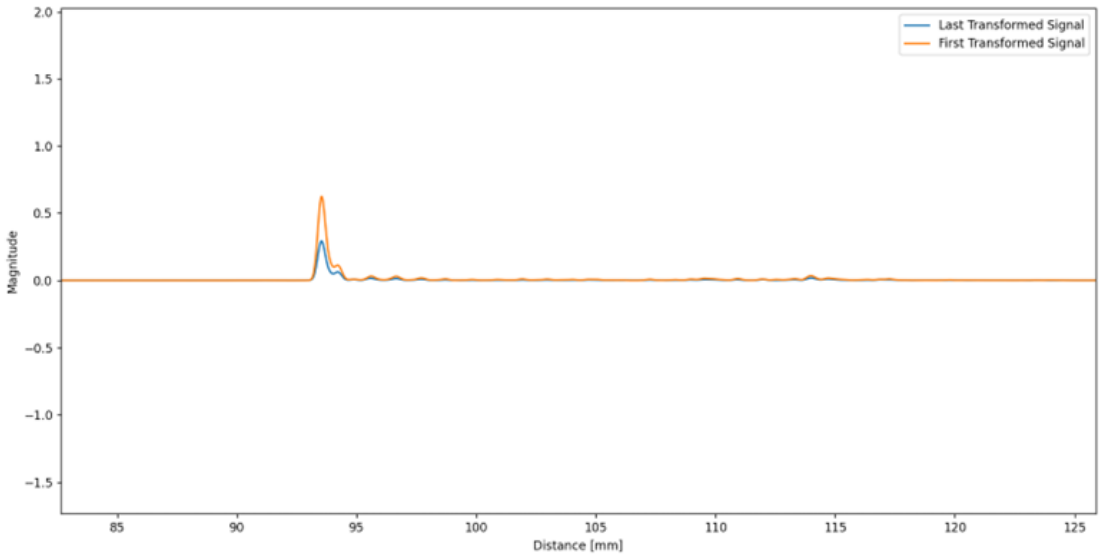

Figure 4.5: Hilbert transforms of the first and last received signals in measurement 4.3. The plot of these signals is focused on the interval between 85 mm and 175 mm.

For the second part of this experiment, we have measured 76 seconds on the same setup, while pouring talcum powder in the aquarium. The pour was an inconsistent dispensing, as we increased the concentration through out the whole period of the measurement.We pour the powder directly in front of the transducer, which is why there might be timestamps displaying a particularly noisy signal. Figure B.2 in the Appendix is an example for it. Interestingly, the 4 MHz frequency is still retrievable as showcased in the Appendix on Figure B.3. Otherwise, after dispersing the particles of the powder evenly, the signal and the associated distance readings are accurate.

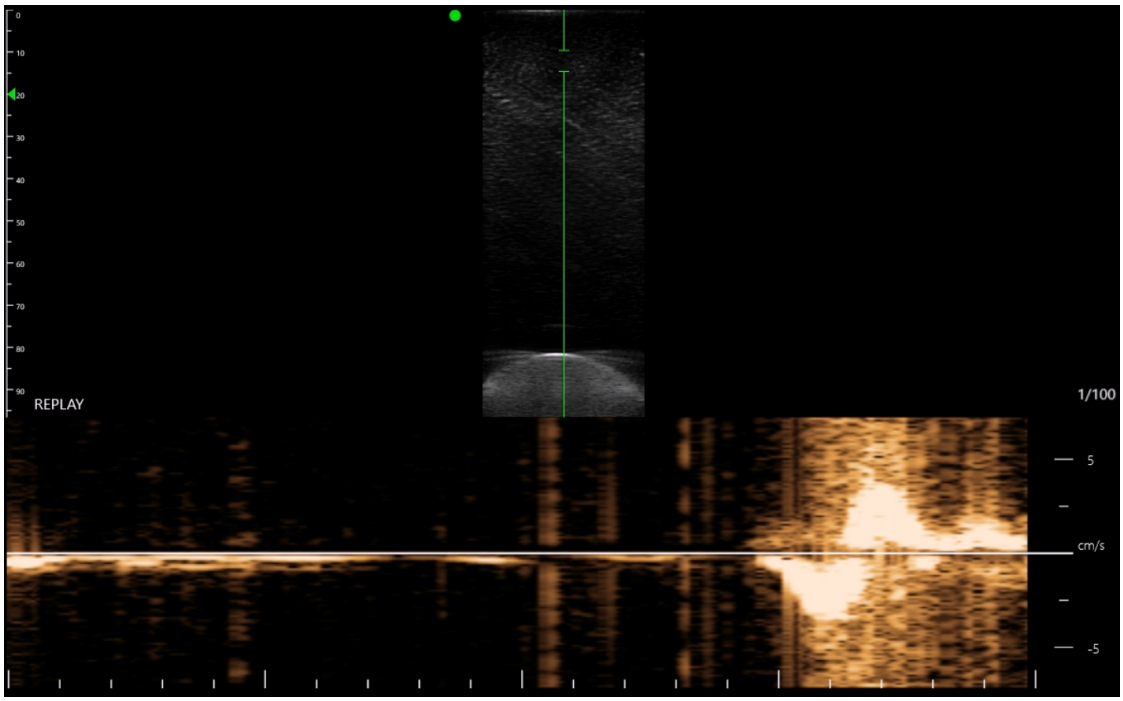

Figure 4.6: Side view image of the wireless ultrasound detection. The green line indicates the ultrasound's aim and its position. Also at the bottom of the figure the Doppler shift is included in brown shades.

The third part involved Doppler ultrasound measurements with the linear array, where we examined whether the flow of water is measurable. The target **3)**, highlighted on the Schematic Setup Figure 3.2, was detectable on the grayscale B-mode image. After switching on the pump the Doppler shift of the transducer frequency appeared, relaxing after the pump was switched off. A still image of the side view of these measurements is shown on Figure 4.6, with the Doppler shift below in brown shades, featuring a noticeable curve that emerges the moment the water pump is switched on.

Chapter 5

Summary

5.1. Problem statement

In addressing the workflow for an ultrasound imaging system, it is imperative to estimate the Echo Excess value (mentioned in equation 2.4), a key determinant of system functionality. However, complications arise due to transmission losses, a concern corroborated by findings in a specific scientific paper.[7] This paper suggests that in scenarios characterized by high turbidity and increased flow rates, traditional sensors may encounter substantial transmission losses. This observation prompts a critical examination of the system's efficacy in challenging conditions. To thoroughly investigate these issues, a well-founded background and well-designed experiments become essential components of the project, aiming to validate or refute the concerns raised in the literature and ensure the robustness of the ultrasound imaging system.

5.2. Results

5.2.1 Demonstrating the workflow

As outlined in Chapter 4, the experiment went well. It confirmed that the script and equations we tested are effective, and the measurements matched our expectations.

5.2.2 Measurements in turbid water

In this measurement, we reduced the water transparency and then measured the distance. Despite the signal remaining readable, it became significantly noisier. However, upon calculating the spectrogram, consistent results were observed in both clear and turbid water conditions.

5.2.3 Measurements in turbid and flowing water conditions

This measurement consisted of three part. The first part showed, that simple flow of water having a regular NTU level has no effect on the measured distance. There were no signs of error. In the second part of the experiment, we have experienced similar results mentioned in a paper [7], when we directly poured the powder in front of the transducer. However, when the particles were evenly distributed, we had a signal, with no errors. Therefore, for in future measurements we do not have to worry about turbid water with a directed flow, only in cases when we for example directly look at stirred up the mud near the bedding.

5.3. Future plans

Looking ahead in the project, our goal is to develop an algorithm utilizing the acquired knowledge to interpret imaging across a spectrum of scenarios and diverse environments. We intend to address environmental challenges by integrating artificial intelligence into sensor systems, paving the way for the foreseeable possibility of generating a real-time 3D view of the environment. This advancement holds promising applications in naval mine-hunting sonars, water rescue operations, disaster management, and various other domains where such a device could prove invaluable.

Bibliography

[1] D. Jung, J. Kim, and G. Byun, "Numerical modeling and simulation technique in time-domain for multibeam echo sounder," *International Journal of Naval Architecture and Ocean Engineering*, vol. 10, no. 2, pp. 225–234, Mar. 2018, ISSN: 2092-6782. DOI: 10.1016/j.ijnaoe.2017.08.004. [Online]. Available: https://www.sciencedirect.com/science/article/pii/S2092678216305179 (visited on 12/13/2023).

[2] EdgeTech, *Application Note: Sidescan Sonar Beamwidth EdgeTech*, 2005. [Online]. Available: https://www.edgetech.com/wp-content/uploads/2019/07/app_note_beamwidth.pdf.

[3] *Analysis of angular resolution and range resolution on multibeam echosounder R2 Sonic 2020 in Port of Tanjung Perak (Surabaya) - ProQuest*, hu. [Online]. Available: https://www.proquest.com/openview/cecde8e1a4ba9b7378a1e2e8208fcf60/1?pq-origsite=gscholar&cbl=4998669 (visited on 12/13/2023).

[4] International Hydrographic Bureau, *MANUAL ON HYDROGRAPHY* (Publication C-13). B.P. 445 - MC 98011 MONACO Cedex: International Hydrographic Bureau, Dec. 2010, vol. 5th edition, Chaoter 3 Depth Estimation. [Online]. Available: www.iho.int.

[5] A. E. Albright Blomberg, A. Austeng, R. E. Hansen, and S. A. V. Synnes, "Improving Sonar Performance in Shallow Water Using Adaptive Beamforming," *IEEE Journal of Oceanic Engineering*, vol. 38, no. 2, pp. 297–307, Apr. 2013, Conference Name: IEEE Journal of Oceanic Engineering, ISSN: 1558-1691. DOI: 10.1109/JOE.2012.2226643. [Online]. Available: https://ieeexplore.ieee.org/document/6401207 (visited on 12/13/2023).

[6] S. D. Richards, "The effect of temperature, pressure, and salinity on sound attenuation in turbid seawater," *The Journal of the Acoustical Society of America*, vol. 103,

no. 1, pp. 205–211, Jan. 1998, ISSN: 0001-4966. DOI: 10.1121/1.421088. [Online]. Available: https://doi.org/10.1121/1.421088 (visited on 12/13/2023).

[7] M. Fisher, M. N. Chowdhury, A. A. Khan, and S. Atamturktur, "An evaluation of scour measurement devices," *Flow Measurement and Instrumentation*, vol. 33, pp. 55–67, Oct. 2013, ISSN: 0955-5986. DOI: 10.1016/j.flowmeasinst.2013.05.001. [Online]. Available: https://www.sciencedirect.com/science/article/pii/S0955598613000666 (visited on 12/13/2023).

[8] *EUT3160*, en. [Online]. Available: http://usultratek.com/EUT3160/ (visited on 12/13/2023).

[9] *Scipy.signal.hilbert — SciPy v1.11.4 Manual*. [Online]. Available: https://docs.scipy.org/doc/scipy/reference/generated/scipy.signal.hilbert.html (visited on 12/13/2023).

[10] *Numpy.fft.fft — NumPy v1.26 Manual*. [Online]. Available: https://numpy.org/doc/stable/reference/generated/numpy.fft.fft.html (visited on 12/13/2023).

[11] *Scipy.signal.spectrogram — SciPy v1.11.4 Manual*. [Online]. Available: https://docs.scipy.org/doc/scipy/reference/generated/scipy.signal.spectrogram.html (visited on 12/13/2023).

[12] P. Allisy-Roberts and J. Williams, "Chapter 9 - imaging with ultrasound," in *Farr's Physics for Medical Imaging (Second Edition)*, P. Allisy-Roberts and J. Williams, Eds., Second Edition, W.B. Saunders, 2008, pp. 147–168, ISBN: 978-0-7020-2844-1. DOI: https://doi.org/10.1016/B978-0-7020-2844-1.50013-2. [Online]. Available: https://www.sciencedirect.com/science/article/pii/B9780702028441500132.

Appendix A

Appendix

The Python script I have used is available with the following link:
https://github.com/csataridominik/TutoredResearchProject01

Appendix B

Appendix

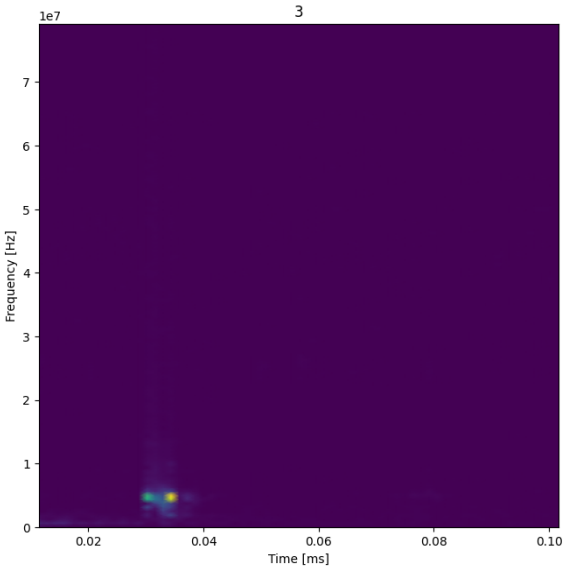

Figure B.1: Spectrogram of the measurement made in Section 4.2. The '3' on top of the figure indicates that it is the 3. received signal's spectrogram

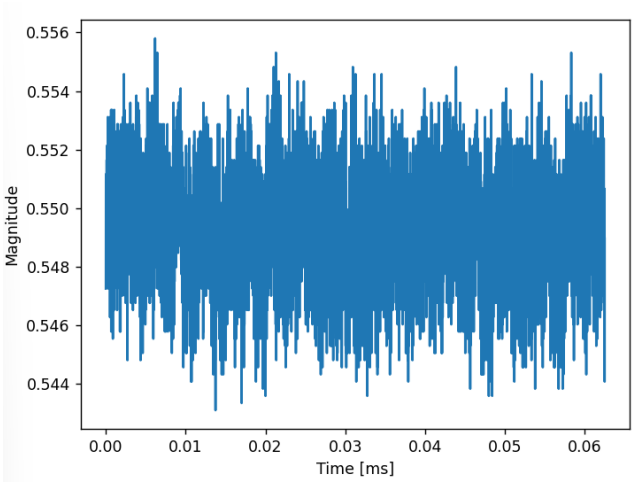

Figure B.2: Noisy RF Signal measured int the second part of the measurement 4.3.

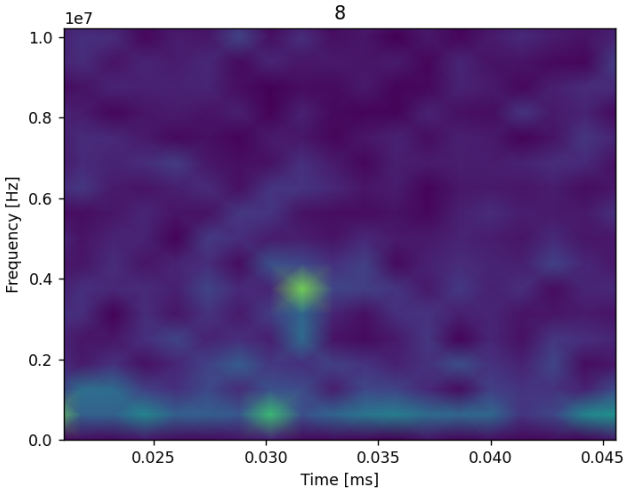

Figure B.3: Spectrogram of the noisy RF Signal measured int the second part of the measurement 4.3. On the top part of the figure '8' indicates that it is the 8th received signal's spectrogram.